

Introduction to geochronology information released in 2011

by

MTD Wingate and CL Kirkland

Introduction

This introduction provides background analytical details for ion microprobe (SHRIMP) U–Pb age determinations released by the Geological Survey of Western Australia (GSWA) as Geochronology Records during 2011. Individual Geochronology Records describe the samples analysed and analytical results obtained, and provide a brief interpretation of these results. The broader geological implications of the data may be published elsewhere. Release of new Geochronology Records to the web (<<http://www.dmp.wa.gov.au/geochron>>) is performed throughout the year as Records are completed.

Most of the samples have been assigned to tectonic or stratigraphic units based on the interpretation of geochronological results and field relationships at the time of publication. These assignments, and the currency of stratigraphic and tectonic units, may subsequently be revised, and up-to-date information should be obtained from the latest GSWA publications.

Analytical procedures

Sample preparation

Rock samples are trimmed of weathered surfaces and secondary veins using a rock saw. The cleaned material is washed, and then crushed to centimetre-size fragments using a customized mechanical jaw-crusher that is disassembled and cleaned prior to the processing of each sample. Between 0.5 and 4 kg of the resulting rock fragments are ground in a low-chromium steel ring-mill, using the minimum grinding time necessary for the resulting powder to pass through a disposable nylon sieve cloth with a mesh size of 400 μm . Very fine particles are removed and discarded from the sieved powder by elutriation, in batches of approximately 300 g, using filtered water under controlled flow conditions (400–2400 ml/min), and a 2000 ml glass funnel apparatus designed and constructed by GSWA's Carlisle laboratory. The remaining fraction is dried overnight in an oven at 90°C, before being split into batches of <150 g. Each batch is then mixed with sodium polytungstate solution ($\text{Na}_6[\text{H}_2\text{W}_{12}\text{O}_{40}] \cdot \text{H}_2\text{O}$), which has a density of about

2.9 g/cm³ at 20°C, in 1000 ml glass separating funnels. The funnels are periodically stirred to facilitate density separation.

The heavy mineral concentrate is drained from each funnel onto a filter paper, washed thoroughly with distilled water and acetone in a Büchner vacuum funnel, and oven-dried overnight at 90°C. Highly magnetic minerals are removed using a hand magnet, followed by one or more passes through a rotating rare earth element magnetic separator, also designed at the Carlisle laboratory. The remaining material is processed using a Frantz isodynamic magnetic separator. For the first pass, a longitudinal tilt of 20°, a transverse tilt of 10°, and a magnet current of 0.2–0.8 A are employed. The non-magnetic fraction from the first pass is reprocessed using higher tilt settings and current values that vary on an individual sample basis. All fractions from each sample are retained in storage.

The resulting non-magnetic fraction is treated with methylene iodide (CH_2I_2), using a sensitive, miniaturized 'double-tube' method (Bastian, 1994). This involves using a 16 mm diameter test tube into which a 1.5 mm diameter constriction has been placed, so that an open, bell-shaped chamber is present at its base. The constriction is small enough that the heavy liquid is held in the upper chamber by its meniscus when the top of the tube is stoppered. The constricted tube is placed into a larger test tube containing methylene iodide, which has a density of about 3.3 g/cm³ at 20°C. The heavy mineral concentrate is carefully poured into the inner tube, the contents are gently stirred, and the inner tube is gently rotated and tilted. Minerals with densities greater than 3.3 g/cm³ fall past the constriction to settle in the outer test tube. When separation is complete, the inner tube is stoppered, slowly lifted out, and the contents washed with acetone onto a filter paper. The purified heavy mineral concentrate in the outer test tube is collected on a second filter paper.

Zircon, monazite, or baddeleyite crystals are then hand-picked from the heavy mineral separate with the aid of a binocular microscope. In general, up to 150–200 representative crystals are selected for igneous and metamorphic rocks, and all grains are picked for sedimentary rocks containing detrital zircons. Crystals are mounted in 25 mm diameter Epofix epoxy disks, and the mount surface polished to expose the grain interiors.

Table 1. Relevant values for ion microprobe reference standards employed at GSWA

| Standard | Mineral | ²³⁸ U (ppm) | ²³² Th (ppm) | ²³⁸ U/ ²⁰⁶ Pb age (Ma) | ²⁰⁷ Pb/ ²⁰⁶ Pb age (Ma) | Reference |
|----------|-------------|---------------------------|----------------------------|---|--|--|
| CZ3 | zircon | 551 | – | 561.5 | – | Pidgeon et al., 1994; Nasdala et al., 2008 |
| Temora 2 | zircon | – | – | 416.8 | – | Black et al., 2004 |
| BR266 | zircon | 909 | – | 559.0 | – | Stern, 2001 |
| OGC1 | zircon | – | – | – | 3 465 | Stern et al., 2009 |
| PBR2 | baddeleyite | – | – | 2 060 | 2 060 | Heaman, 2008 |
| India | monazite | 2 890 | 36 946 | 509 | – | PD Kinny and C Clark, 2010, pers. comm. |
| GM3 | monazite | 488 | 6300 | 488 | 487.1 | Kennedy and Kinny, 2004 |

NOTE: OGC1 is the zircon standard obtained by Curtin University from the same rock from which standard OG1 was described by Stern et al. (2009)

Each mount typically contains minerals from one, two, or three different samples, together with several crystals or crystal fragments of reference materials (details in Table 1). U–Pb calibration standards for zircon include CZ3, Temora2, and BR266, whereas PBR2 is used for baddeleyite. To monitor the accuracy of ²⁰⁷Pb/²⁰⁶Pb ratios in zircon and baddeleyite analyses, zircon crystals from sample OGC1 of the 3465 Ma Owens Gully Diorite are included on each mount. The CZ3 or BR266 zircon standard is used for concentration calibration. Several zircons with high ²³⁸U and Pb concentrations are also added to each zircon or baddeleyite mount to facilitate setup of the mass peaks on the ion microprobe. For monazite analysis, the India monazite standard is used for U–Pb calibration, whereas the GM3 monazite standard is used to monitor the accuracy of ²⁰⁷Pb/²⁰⁶Pb ratios.

Mineral imaging and target selection

Each mount is photographed in transmitted light, reflected light, and in reflected light using a differential interference contrast (Nomarski) filter, at a magnification of 70–150x. The mount is then ultrasonically cleaned in ethanol, petroleum ether, and detergent (Decon), then rinsed in distilled and deionized water, and dried in an oven at 60°C. The polished surface of the mount is then coated evaporatively with high-purity gold to a thickness of about 40 nm, to achieve an edge-to-edge resistance of 15–25 ohms.

To reveal the internal structures of zircons, cathodoluminescence (CL) imaging of all zircons on the mount is undertaken prior to analysis, using a Philips XL30 scanning electron microscope (SEM) fitted with a KE Developments CL detector, located in the Department of Imaging and Applied Physics at Curtin University. The instrument is typically operated with an accelerating voltage of 12 keV. High-definition CL images are obtained at a resolution of 1936 lines/scan at 60 ms duration/line. For each sample, approximately 4–10 images are acquired at magnifications in the range 70–150x, providing complete coverage of the mounted crystals. Backscattered-electron (BSE) images, also obtained using the Philips XL30 SEM, are employed to image baddeleyite and monazite. Mineral crystals to be analysed are selected

based on their combined CL (or BSE), reflected-light, and transmitted-light characteristics.

SHRIMP U–Pb analysis

Operating procedures for uranium, thorium, and lead isotopic measurements on zircon are based on those described by Compston et al. (1984) and Clauoué-Long et al. (1995), with modifications summarized by Williams (1998). Procedures for baddeleyite follow Wingate et al. (1998). Procedures for monazite analysis follow Williams et al. (1996), with modifications by Kinny (1997). For zircon and baddeleyite analysis, a 20–30 µm diameter primary beam of O₂⁻ ions at 10 keV, purified by means of a Wien filter, is employed to sputter secondary ions from the surface of each target mineral. The net primary ion current, as measured leaving the sample, is typically between 1.5 and 3.5 nA. Secondary ions are accelerated to 10 keV, energy-filtered by passage through a cylindrical 85° electrostatic analyser with a turning radius of 1.27 m, and mass-filtered using a 72.5° magnet sector with a turning radius of 1 m. Secondary ions are counted by switching the magnetic field to direct the secondary ion beam into an electron multiplier, used in pulse-counting mode. During the analytical session, the secondary ion analyser is set to a mass resolution of ≥5000 (1% peak-height definition), which is sufficient to resolve lead isotopes from most potential molecular interferences. The magnetic field is cycled several times to select isotopic masses in the following sequence: 196 (species [⁹⁰Zr₂¹⁶O]⁺, count time 2 s), 204 (²⁰⁴Pb⁺, 10 s), 204.1 (background, 10 s), 206 (²⁰⁶Pb⁺, 10 s), 207 (²⁰⁷Pb⁺, 20–40 s), 208 (²⁰⁸Pb⁺, 10 s), 238 (²³⁸U⁺, 5 s), 248 ([²³²Th¹⁶O]⁺, 5 s), and 254 ([²³⁸U¹⁶O]⁺, 2 s). Data are collected for six cycles through the mass stations for the dating of minerals from igneous or metamorphic rocks. This is reduced to five cycles for the dating of detrital zircons from sedimentary rocks in order to maximize the number of crystals that can be analysed during the session.

SHRIMP monazite analyses are similar to those of zircon, although a lower-intensity primary ion beam can be used, owing to higher secondary-ion count rates on the species of interest. Typically, a 5–10 µm diameter primary beam, with an intensity of ~0.5 nA, is employed.

Ion microprobe analyses of monazite are affected by an uneven background spectrum of scattered ions (Kinny, 1997), which can be reduced effectively by use of the SHRIMP retardation lens system, which is set at c. 10 kV. This discriminates against low-energy ions entering the collector. Each analysis consists of six cycles through the isotopic masses in the following sequence: 202 (species $[^{139}\text{La}^{31}\text{P}^{16}\text{O}_2]^+$ count time 2 s), 203 ($[^{140}\text{Ce}^{31}\text{P}^{16}\text{O}_2]^+$, 2 s), 204 ($^{204}\text{Pb}^+$ 10 s), 204.1 (background, 10 s), 206 ($^{206}\text{Pb}^+$, 10 s), 207 ($^{207}\text{Pb}^+$, 30 s), 208 ($^{208}\text{Pb}^+$, 5 s), 232 ($^{232}\text{Th}^+$, 5 s), 254 ($[^{238}\text{U}^{16}\text{O}]^+$, 5 s), 264 ($[^{232}\text{Th}^{16}\text{O}_2]^+$, 2 s), and 270 ($[^{238}\text{U}^{16}\text{O}_2]^+$, 3 s).

Data reduction

SHRIMP U–Pb zircon, baddeleyite, and monazite data are reduced using SQUID 2.50 and Isoplot 3.71 (add-ins for Microsoft Excel; Ludwig, 2003, 2009) with decay constants recommended by Steiger and Jäger (1977). Ratios of $^{206}\text{Pb}^+ / ^{238}\text{U}^+$ in zircon are calibrated to the known $^{206}\text{Pb} / ^{238}\text{U}$ of the zircon standard (Table 1), using a power-law relationship between $^{206}\text{Pb}^+ / ^{238}\text{U}^+$ and UO^+ / U^+ , with a fixed exponent of 2.0 (determined empirically from measurements of zircon standards over several years; Claué-Long et al., 1995). Data compilation and initial visualization are conducted using in-house Microsoft Excel macros. In most cases, data are corrected for the presence of common Pb using measured $^{204}\text{Pb} / ^{206}\text{Pb}$ (Compston et al., 1984). An average crustal composition (Stacey and Kramers, 1975), appropriate to the age of the mineral, is assumed, although in most cases, corrections are sufficiently small to be insensitive to the choice of common-Pb composition. Prior to analysis, each site is cleaned by rastering the primary ion beam over the area for two to four minutes. Subsequently, $^{204}\text{Pb}^+$ counts for most analyses remain low and constant, and show no tendency to decrease over the course of a 12–16 minute analysis, suggesting that common Pb is mainly inherent to the mineral, rather than surface-related.

In a minority of cases, mainly in relatively young (Mesoproterozoic and younger), low-uranium zircons, 204-corrected $^{207}\text{Pb}^* / ^{206}\text{Pb}^*$ (Pb^* indicates radiogenic Pb) ratios are observed to correlate with their common-Pb corrections (i.e. the fraction (f_{204}) of common ^{206}Pb in total ^{206}Pb), indicating that the corrections using ^{204}Pb are inaccurate for some or all analyses. This can occur when background counts are similar in magnitude to those for $^{204}\text{Pb}^+$. In these cases, the 204-correction is abandoned in favour of a regression from initial Pb. This method assumes that the total Pb is a two-component mixture of common and radiogenic Pb, and that both the U–Pb and Pb–Pb isotopic systems are concordant. In this circumstance, the analyses will lie (by amounts proportional to their common-Pb contents) along a mixing line between initial $^{207}\text{Pb} / ^{206}\text{Pb}$ (calculated according to the model of Stacey and Kramers, 1975) and radiogenic Pb, on concordia. The analyses of all minerals of the same age will lie within error of a single regression line anchored at initial Pb; data falling significantly to the left of the mixing line suggest the presence of xenocrystic material, whereas dispersion to the right may indicate ancient or recent radiogenic-Pb loss. The mean date is determined from the lower intercept of the mixing line with the concordia curve.

In cases where the 204-correction is inaccurate, dispersion in the data suggests that zircon growth occurred over an extended interval of time, and the data can be assumed to be essentially concordant, the ‘207-method’ of common-Pb correction may be applied. This procedure extrapolates each analysis along a common-Pb mixing line to the concordia curve to yield the radiogenic $^{238}\text{U} / ^{206}\text{Pb}^*$ date.

Ratios of $^{238}\text{U} / ^{206}\text{Pb}^*$ measured in baddeleyite by ion microprobe have been shown to vary significantly and systematically with the relative orientation of the baddeleyite crystal structure and the direction of the primary ion beam (Wingate and Compston, 2000). Reliable and precise dates can therefore only be determined from $^{207}\text{Pb}^* / ^{206}\text{Pb}^*$ ratios, which are unaffected by this phenomenon (Wingate et al., 1998), although the $^{238}\text{U} / ^{206}\text{Pb}^*$ ratios can still be used in a semi-quantitative manner for assessing the concordance of results. Common-Pb correction in baddeleyite employs either ^{204}Pb , as with zircon, or the ‘208-method’, whereby the proportion of common ^{206}Pb in measured ^{206}Pb (referred to as f_{208}) is determined from the difference between the measured $^{208}\text{Pb} / ^{206}\text{Pb}$ ratio and the radiogenic ratio expected for the age and measured $^{232}\text{Th} / ^{238}\text{U}$ of the mineral (Hinthorne et al., 1979; Compston et al., 1984; Wingate et al., 1998). The 208-method is generally only applicable to minerals (typically baddeleyite and some zircons) having low $^{232}\text{Th} / ^{238}\text{U}$, and may be employed in cases where it provides higher precision and lower dispersion than correction using ^{204}Pb .

Ratios of $^{206}\text{Pb}^+ / ^{238}\text{U}^+$ in monazite are calibrated to the known $^{206}\text{Pb} / ^{238}\text{U}$ of the monazite standard (Table 1) using a linear relationship between $^{206}\text{Pb}^+ / \text{UO}_2^+$ and $\text{UO}^+ / \text{UO}_2^+$ (Kinny, 1997). Monazite generates an unresolvable isobaric interference on $^{204}\text{Pb}^+$, which may be $(^{232}\text{Th}^{144}\text{Nd}^{16}\text{O}_2)^{++}$ (Ireland et al., 1999; Kirkland et al., 2009). This interference has been observed to correlate with thorium content (Kinny, 1997). Excess $^{204}\text{Pb}^+$ counts are corrected against the India monazite standard assuming $^{206}\text{Pb} / ^{238}\text{U} - ^{207}\text{Pb} / ^{235}\text{U}$ age-concordance of the standard at a known thorium concentration. Fractionation of the $^{207}\text{Pb} / ^{206}\text{Pb}$ ratio is typically observed when the retardation lens system is at operating voltage during monazite analysis. Fractionation of the $^{207}\text{Pb} / ^{206}\text{Pb}$ ratio is monitored and corrections can be made, if necessary, by reference to the GM3 monazite standard. Uncertainties associated with this correction are added in quadrature to the uncertainties of $^{207}\text{Pb}^* / ^{206}\text{Pb}^*$ ratios and dates.

Uncertainties assigned to all isotopic ratios and dates for individual analyses reflect contributions arising from counting statistics and common-Pb correction. Ratios and dates based on $^{238}\text{U} / ^{206}\text{Pb}^*$ include an external ‘spot-to-spot’ uncertainty, related to the reproducibility of the standard $^{238}\text{U} / ^{206}\text{Pb}^*$ measurements (for most sessions this is taken to be a minimum of 0.50% (1σ)). The internal uncertainty arising from calibration against the reference standard is also included in individual $^{238}\text{U} / ^{206}\text{Pb}^*$ ratios and dates reported in data tables. In rare cases, significant secular drift of standard $^{238}\text{U} / ^{206}\text{Pb}^*$ dates during an analytical session may be addressed by fitting a LOWESS curve (Cleveland, 1979), as implemented in the program Squid 2.50 (Ludwig, 2009). Details of both the

external ‘spot-to-spot’ and internal calibration uncertainties are reported in the Geochronology Record for each sample.

Data interpretation

Weighted mean dates are determined for groups of analyses by weighting each $^{207}\text{Pb}^*/^{206}\text{Pb}^*$ or $^{238}\text{U}/^{206}\text{Pb}^*$ date by the inverse of its variance (the square of its $1\sigma_i$ analytical uncertainty). Dispersion of results beyond their individual analytical uncertainties ($2.5\sigma_i$) suggests the presence of geological sources of uncertainty (potentially arising from the inclusion of analyses of slightly older xenocrysts, and/or the inclusion of analyses of zircons that may have lost radiogenic Pb).

For most samples, in the case of dispersed data, dates lying furthest from the weighted mean value are excluded progressively from the group until all remaining analyses are within $\pm 2.5\sigma_i$ of the weighted mean value. For some samples, it may not be possible to confidently attribute dispersion to either the presence of xenocrystic material or to minor loss of radiogenic Pb, and it may be reasonable to retain some dates that differ from the weighted mean by amounts in excess of the $2.5\sigma_i$ limits. Weighted mean dates are reported with 95% confidence intervals, defined as the 1σ internal uncertainty of the weighted mean $^{207}\text{Pb}^*/^{206}\text{Pb}^*$ (or $^{238}\text{U}/^{206}\text{Pb}^*$) ratio or date, multiplied by the square root of the MSWD and by Student's *t* for $n-1$ degrees of freedom. As noted above, the uncertainties of weighted mean $^{238}\text{U}/^{206}\text{Pb}^*$ dates also include reproducibility and calibration uncertainties.

In cases where the true location of the mean data point can be assumed to fall on the concordia curve, it is possible to calculate a ‘concordia age’ (Ludwig, 1998), which makes the best use of all $^{207}\text{Pb}^*/^{206}\text{Pb}^*$ and $^{238}\text{U}/^{206}\text{Pb}^*$ ratios. This approach will typically yield a more precise mean age than can be obtained using either ratio alone, and also yields an objective and quantitative measure of concordance.

Data presentation

Both the $^{238}\text{U}/^{206}\text{Pb}$ and $^{207}\text{Pb}/^{206}\text{Pb}$ ratios (not corrected for common Pb), and the $^{238}\text{U}/^{206}\text{Pb}^*$ and $^{207}\text{Pb}^*/^{206}\text{Pb}^*$ ratios (common-Pb corrected), are listed in data tables. Uncertainties in data tables and error bars in figures are at the 1σ level. Stated sample numbers are GSWA sample numbers, unless mentioned otherwise. Within the text, capitalized names refer to standard 1:250 000 and 1:100 000 map sheets; where 1:100 000 and 1:250 000 map sheets have the same name, the 1:100 000 sheet is implied unless otherwise indicated.

Locality coordinates for the majority of samples were obtained using a hand-held Global Positioning System (GPS) receiver, and are accurate to better than ± 100 m. All coordinates use the World Geodetic System 1984 (WGS 84), which, for most practical purposes, is the same as the Geocentric Datum of Australia (GDA 94).

U–Pb data are presented using ‘inverse’ or ‘Tera–Wasserburg’ concordia diagrams (Tera and Wasserburg, 1972). These diagrams have several advantages over

‘conventional’ concordia diagrams (Wetherill, 1956) for ion microprobe analyses. The two main age-sensitive ratios measured using the SHRIMP, $^{207}\text{Pb}^*/^{206}\text{Pb}^*$ and $^{238}\text{U}/^{206}\text{Pb}^*$, are plotted directly on Tera–Wasserburg diagrams, whereas conventional diagrams use $^{206}\text{Pb}^*/^{238}\text{U}$ and $^{207}\text{Pb}^*/^{235}\text{U}$. However, ^{235}U is not directly measured using the SHRIMP, and conventional diagrams do not show $^{207}\text{Pb}^*/^{206}\text{Pb}^*$ ratios, which are the most sensitive indicator of age for minerals >1000 Ma. In addition, Tera–Wasserburg diagrams avoid the strong correlation of uncertainties that visually ‘skews’ data on a conventional diagram. Tera–Wasserburg diagrams also facilitate the processing of data without explicit correction for common Pb, which is useful in cases where the ^{204}Pb -based common-Pb correction is inaccurate.

In addition to presentation on concordia diagrams, dates obtained for zircons from sedimentary rock samples are also displayed on combined probability density and histogram plots. These are used to illustrate the distribution of zircon dates (age spectrum). These diagrams present two cumulative probability density curves: one includes all analyses, and the other includes only those data less than 5% or 10% discordant. The height and width of each age peak is proportional to the number and precision of data points making up the peak. The integrated histogram shows the number of analyses in each peak. Dates for Mesoproterozoic and older detrital zircons are generally based on $^{207}\text{Pb}^*/^{206}\text{Pb}^*$ ratios, whereas those for younger minerals are based on $^{238}\text{U}/^{206}\text{Pb}^*$ ratios. The precise age at which the change is made from one ratio to the other is generally between about 800 and 1000 Ma, and is determined from the age characteristics for each sample.

Abbreviations and formulae used in Geochronology Records

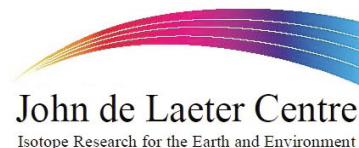
Pb* = radiogenic Pb

f_{204} (%) = $100 \times (\text{common } ^{206}\text{Pb}/\text{total } ^{206}\text{Pb})$, assessed using measured $^{204}\text{Pb}/^{206}\text{Pb}$

f_{208} (%) = $100 \times (\text{common } ^{206}\text{Pb}/\text{total } ^{206}\text{Pb})$, assessed using measured $^{208}\text{Pb}/^{206}\text{Pb}$, $^{232}\text{Th}/^{238}\text{U}$, and date

Discordance (%) = $100 \times [1 - (^{238}\text{U}/^{206}\text{Pb} \text{ date}) / (^{207}\text{Pb}^*/^{206}\text{Pb}^* \text{ date})]$

Acknowledgement



U–Pb measurements are conducted using the SHRIMP ion microprobes at the John de Laeter Centre of Mass Spectrometry at Curtin University, in Perth, Western Australia.

References

- Bastian, LV 1994, The dune systems of the Swan coastal plain: subdivision based on mineral trends in the surface soils: Chemistry Centre of Western Australia, Report of Investigation 41, 45p.
- Black, LP, Kamo, SL, Allen, CM, Davis, DW, Aleinikoff, JN, Valley, JW, Mundil, R, Campbell, IH, Korsch, RJ, Williams, IS and Foudoulis, C 2004, Improved $^{206}\text{Pb}/^{238}\text{U}$ microprobe geochronology by the monitoring of a trace element related matrix effect: SHRIMP, ID-TIMS, ELA-ICP-MS, and oxygen isotope documentation for a series of zircon standards: *Chemical Geology*, v. 205, p. 115–140.
- Claoué-Long, JC, Compston, W, Roberts, J and Fanning, CM 1995, Two Carboniferous ages: a comparison of SHRIMP zircon dating with conventional zircon ages and $^{40}\text{Ar}/^{39}\text{Ar}$ analysis, in *Time Scales and Global Stratigraphic Correlation edited by WA Berggren, DV Kent, M-P Aubrey, and J Hardenbol*: Society for Sedimentary Geology, Special Publication 54, p. 3–21.
- Cleveland, WS 1979, Robust, locally weighted regression and smoothing scatterplots: *Journal of the American Statistical Association*, v. 74, p. 829–836.
- Compston, W, Williams, IS and Meyer, C 1984, U–Pb geochronology of zircons from lunar breccia 73217 using a sensitive high mass-resolution ion microprobe: *Journal of Geophysical Research*, v. 89, p. B252–B534.
- Heaman, LM 2008, The application of U–Pb geochronology to mafic, ultramafic and alkaline rocks: an evaluation of three mineral standards: *Chemical Geology*, v. 261, p. 43–52.
- Hinthorne, JR, Andersen, CA, Conrad, RL and Lovering, JF 1979, Single-grain $^{207}\text{Pb}/^{206}\text{Pb}$ and U/Pb age determinations with a 10 mm spatial resolution using the ion microprobe mass analyzer (IMMA): *Chemical Geology*, v. 25, p. 271–303.
- Ireland, TR, Wooden, JL, Persing, H and Ito, B 1999, Geological applications and analytical development of the SHRIMP-RG: *EOS Transactions, American Geophysical Union* 80, p. F1117.
- Kennedy, A and Kinny, PD 2004, Identifying inter- and intra-laboratory SIMS monazite standards: SHRIMP workshop abstract volume, Hiroshima, Japan, p. 11–14.
- Kinny, PD 1997, Users' guide to U–Th–Pb dating of titanite, perovskite, monazite, and baddeleyite using the WA SHRIMP: Curtin University of Technology, School of Physical Sciences, Report SPS693/1997/AP72, 21p.
- Kirkland, CL, Whitehouse, MJ and Slagstad, T 2009, Fluid-assisted zircon and monazite growth within a shear zone; a case study from Finnmark, Arctic Norway: *Contributions to Mineralogy and Petrology*, v. 158, p. 637–657.
- Ludwig, KR 1998, On the treatment of concordant uranium–lead ages: *Geochimica et Cosmochimica Acta*, v. 62, p. 665–676.
- Ludwig, KR 2003, Isoplot 3.00: A geochronological toolkit for Microsoft Excel: Berkeley Geochronology Centre, Special Publication 4, 70p.
- Ludwig, KR 2009, Squid 2.50, A User's Manual: Berkeley Geochronology Centre, Berkeley, California, USA, 95p. (unpublished report).
- Nasdala, L, Hofmeister, W, Norberg, N, Mattinson, JM, Corfu, F, Dörr, W, Kamo, SL, Kennedy, AK, Kronz, A, Reiners, PW, Frei, D, Kosler, J, Wan, Y, Götze, J, Häger, T, Kröner, A and Valley, JW 2008, Zircon M257 — a homogeneous natural reference material for the ion microprobe U–Pb analysis of zircon: *Geostandards and Geoanalytical Research*, v. 32, p. 247–265.
- Pidgeon, RT, Furfaro, D, Kennedy, AK, Nemchin, AA and Van Bronswijk, W 1994, Calibration of zircon standards for the Curtin SHRIMP II, in *Eighth International Conference on Geochronology, Cosmochronology, and Isotope Geology — Abstracts: United States Geological Survey, Circular 1107*, p. 251.
- Stacey, JS and Kramers, JD 1975, Approximation of terrestrial lead isotope evolution by a two-stage model: *Earth and Planetary Science Letters*, v. 26, p. 207–221.
- Steiger, RH and Jäger, E 1977, Subcommittee on geochronology: convention on the use of decay constants in geo- and cosmochronology: *Earth and Planetary Science Letters*, v. 36, p. 359–362.
- Stern, RA 2001, A new isotopic and trace-element standard for the ion microprobe: preliminary thermal ionization mass spectrometry (TIMS) U–Pb and electron-microprobe data: Geological Survey of Canada, Radiogenic Age and Isotopic Studies, Report 14, Current Research 2001-F1, 11p.
- Stern, RA, Bodorkos, S, Kamo, SL, Hickman, AH and Corfu, F 2009, Measurement of SIMS instrumental mass fractionation of Pb isotopes during zircon dating: *Geostandards and Geoanalytical Research*, v. 33, p. 145–168.
- Tera, F and Wasserburg, GJ 1972, U–Th–Pb systematics in three Apollo 14 basalts and the problem of initial Pb in lunar rocks: *Earth and Planetary Science letters*, v. 14, p. 281–304.
- Wetherill, GW 1956, Discordant uranium–lead ages: *Transactions of the American Geophysical Union*, v. 37, p. 320–326.
- Wingate, MTD, Campbell, IH, Compston, W and Gibson, GM 1998, Ion microprobe U–Pb ages for Neoproterozoic basaltic magmatism in south-central Australia and implications for the breakup of Rodinia: *Precambrian Research*, v. 87, p. 135–159.
- Wingate, MTD and Compston, W 2000, Crystal orientation effects during ion microprobe U–Pb analysis of baddeleyite: *Chemical Geology*, v. 168, p. 75–97.
- Williams, IS, Buick, IS and Cartwright, I 1996, An extended episode of early Mesoproterozoic metamorphic fluid flow in the Reynolds Range, central Australia: *Journal of Metamorphic Geology*, v. 14, p. 29–47.
- Williams, IS 1998, U–Th–Pb geochronology by ion microprobe, in *Applications of Microanalytical Techniques to Understanding Mineralizing Processes edited by MA McKibben, WC Shanks III, WI Ridley*: *Reviews in Economic Geology*, v. 7, p. 1–35.

Recommended reference for this publication

- Wingate, MTD and Kirkland, CL 2011, Introduction to geochronology information released in 2011: Geological Survey of Western Australia, 5p.